Structural Basis for Low Catalytic Activity in Lys49 Phospholipases A2—A Hypothesis: The Crystal Structure of Piratoxin II Complexed to Fatty Acid[†,‡]

Wen-Hwa Lee,[#,§] Maria Teresa da Silva Giotto,[||] Sérgio Marangoni,[⊥] Marcos H. Toyama,[⊥] Igor Polikarpov,[*,#] and Richard C. Garratt[*,||]

Laboratório Nacional de Luz Síncrotron, Caixa Postal 6192, 13083-970 Campinas, São Paulo, Brazil, Departamento de Genética e Evolução, Instituto de Biologia, UNICAMP, Caixa Postal 6109, 13083-970 Campinas, São Paulo, Brazil, Instituto de Física de São Carlos, Universidade de São Paulo, Caixa Postal 369, 13560-970 São Carlos, São Paulo, Brazil, and Departamento de Bioquímica, Instituto de Biologia, UNICAMP, Caixa Postal 6109, 13083-970 Campinas, São Paulo, Brazil

Received May 8, 2000; Revised Manuscript Received August 14, 2000

ABSTRACT: Asp49 plays a fundamental role in supporting catalysis by phospholipases A2 by coordinating the calcium ion which aids in the stabilization of the tetrahedral intermediate. In several myotoxins from the venoms of *Viperidae* snakes, this aspartic acid is substituted by lysine. The loss of calcium binding capacity by these mutants has become regarded as the standard explanation for their greatly reduced or nonexistent phopholipolytic activity. Here we describe the crystal structure of one such Lys49 PLA2, piratoxin-II, in which a fatty acid molecule is observed within the substrate channel. This suggests that such toxins may be active enzymes in which catalysis is interrupted at the stage of substrate release. Comparison of the present structure with other PLA2s, both active and inactive, identifies Lys122 as one of the likely causes of the increased affinity for fatty acid in Lys49 enzymes. Its interaction with the mainchain carbonyl of Cys29 is expected to lead to hyperpolarization of the peptide bond between residues 29 and 30 leading to an increased affinity for the fatty acid headgroup. This strongly bound fatty acid may serve as an anchor to secure the toxin within the membrane thus facilitating its pathological effects.

The phospholipases A_2 (PLA_2)[1] are probably among the most widely studied of all enzyme families both in terms of their structural characteristics and catalytic properties. From a structural perspective, enzymes isolated from the venom of serpents (*1*−*11*) and insects (*12*) as well as from mammalian sources [pancreas (*13*, *14*) and synovial fluid (*15*, *16*)] have been the subject of intense investigation by both X-ray diffraction and more recently multidimensional NMR (*17*). The latter has been exploited for the study of phospholipase A_2 structure both in solution and at the membrane interface in the form of complexes with micelles (*18*), revealing important aspects of interfacial catalysis for which PLA_2 remains a fundamental paradigm (*19*). Recently, theoretical techniques such as molecular dynamics simulations at membrane boundaries (*20*) have also been used to complement this wealth of experimental data.

Crystallographic studies have found application in the rational design of potent inhibitors of human non-pancreatic secretory PLA_2 (*21*) and the use of transition state and substrate analogues has also made important contributions to our current understanding of the catalytic mechanism (*4*, *12*, *16*, *22*). Such studies have been more recently complemented by site-directed mutagenesis in which the role of individual residues of the active site and the so-called hydrogen-bonding network have been specifically probed (*23*−*25*).

The basis of our current view of the catalytic mechanism was originally inferred by Veiheij et al. (*26*) and subsequently refined by Scott et al. (*27*) on the basis of crystal structures of complexes with the transition state analogue L-1-*O*-octyl-2-heptylphosphonyl-*sn*-glycero-3-phosphoethanolamine. The catalytic histidine (His48) aided by Asp99, is believed to activate a water molecule to promote nucleophilic attack on the *sn-2* position of the phospholipid substrate, in a manner similar to that proposed for serine proteases (*28*). Fundamental to this process is the stabilization of the oxyanion on the tetrahedral intermediate by the essential calcium cofactor together with the backbone amide NH of residue 30 [numbering according to Renetseder et al. (*29*)]. Scott et al. also infer the need for a supplementary electrophile to polarize the peptide bond in which NH30 participates. More recently, Rogers et al. (*30*) have proposed an alternative to the current consensus by suggesting that two different water

[†] This work was financially supported by the Brazilian funding bodies FAPESP, CAPES, CNPq, and FINEP (PRONEX).

[‡] Atomic coordinates have been deposited in the Protein Data Bank under code 1QLL.

* To whom correspondence should be addressed: R. C. Garratt, Dept. Física e Informática, Inst. Física de São Carlos, Univ. de São Paulo, Caixa Postal 369, São Carlos/SP, Brazil, CEP-13560-970, telephone: +55 16 273 9874, fax: +55 16 273 9881, e-mail: richard@if.sc.usp.br or I. Polikarpov, Lab. Nacional Luz Síncrotron LNLS, Caixa Postal 6192, Campinas/SP, Brazil, CEP-13083-970, telephone: +55 19 287 4520, fax: +55 19 287 4632, e-mail: igor@lnls.br.

[#] Laboratório Nacional de Luz Síncrotron.

[§] Departamento de Genética e Evolução, Instituto de Biologia, UNICAMP.

[||] Universidade de São Paulo.

[⊥] Departamento de Bioquímica, Instituto de Biologia, UNICAMP.

[1] Abbreviations: PLA_2, phospholipase A_2; PrTX-II, piratoxin II; PEG, polyethylene glycol; App, *Agkistrodon piscivorus piscivorus*; ASPC, 2-arachidonoyl-1-stearoyl-L-3-phosphatidylcholine; CCP4, collaborative computational project 4.

10.1021/bi0010470 CCC: $20.00
Published on Web 12/12/2000

molecules are involved in the formation and breakdown, respectively, of the tetrahedral intermediate and that the former is activated by the Ca^{2+} ion rather than the catalytic histidine.

Over the past few years, much attention has been directed toward the study of naturally occurring myotoxic PLA_2 homologues isolated from the venom of snakes from the *Viperidae* family, in which one of the ligands of the essential calcium ion, Asp49, has been replaced by lysine (*31*). Originally described by Maraganore (*32*), these variants have been widely described as catalytically inactive as a consequence of their incapacity to bind the essential calcium cofactor and thus stabilize the tetrahedral intermediate (*33*, *34*). However, there have been recent reports that Lys49 variants do indeed present limited catalytic activity (*35*−*37*) and both sequence analysis (*38*) and X-ray diffraction studies (*39*−*46*) show that all such PLA_2 homologues have conserved all other important aspects of the catalytic machinery, including His48, Asp99, Tyr52, Tyr73, the catalytic water and the remainder of the hydrogen-bonding network. In the current work, we specifically address this apparent paradox and describe the crystal structure of Piratoxin II, a Lys49 PLA_2 homologue isolated from the venom of *Bothrops pirajai*. Surprisingly, the structure reveals the presence of nonprotein electron density within the hydrophobic substrate-binding channel that can be readily interpreted as the fatty acid product of catalysis. On the basis of this and other Lys49 structures, we propose an additional or alternative explanation for their apparent lack of activity which is based on a failure of product release.

MATERIALS AND METHODS

Piratoxin II (PrTX-II) from *B. pirajai* whole venom was isolated by semipreparative reverse phase HPLC, as described previously (*47*). Initial screening of crystallization conditions was performed by vapor-diffusion in hanging-drops using sparse-matrix sampling (*48*), which identified a single condition that yielded flat platelike crystals (*49*). The best crystals were obtained at 277 K using protein dissolved in water at 20 mg/mL mixed with an equal volume of a well solution composed of 28% PEG 3350, 0.25M Li_2SO_4, and 0.1M Tris-HCl, pH 8.5, and grew after 40 days to maximum dimensions of $0.1 \times 0.1 \times 0.02$ mm^3. X-ray diffraction data from these crystals were collected at the Protein Crystallography (PCr) beamline (*50*, *51*) at the National Laboratory of Synchrotron Light (LNLS) located in Campinas, Brazil. The wavelength of the synchrotron radiation was set to 1.38 Å, and all diffraction images were collected on a MAR345 image plate. A total of 58 scanning oscillation images were recorded in 1.5° steps (87° total rotation) and processed to 2.04 Å using DENZO and ScalePack from the HKL program suite (*52*). The crystals were determined to belong to the space group $P2_1$ with cell parameters $a = 46.19$ Å, $b = 60.36$ Å, $c = 58.74$ Å, and $\beta = 96.05°$. Crystallization and data collection statistics for PrTX-II are presented in Table 1.

The PrTX-II crystal structure was solved by molecular replacement using the program *AMoRe* (*53*). The search model used was that of a single monomer of the PLA_2 dimer from *Bothrops asper* [PDB ID code 1CLP (*41*)] with which PrTX-II shares 96% sequence identity and included all main chain and side chain atoms. The rotation and translation searches were performed using all data between 10.0 and 3.0 Å resolution. Two molecules of PrTX-II were located in the asymmetric unit yielding a correlation coefficient of 63.4% and an *R*-factor of 38.9% after 10 cycles of rigid body refinement. The crystal packing of the molecules was manually inspected and the model subsequently was subjected to maximum likelihood refinement with isotropic B-factors using the program REFMAC (*54*) after substitution of the necessary side chains (*55*). Consecutive cycles of refinement were performed and the electron density maps of the best model [as evaluated by the conventional *R* and R_{free} factors (*56*)] after each cycle were examined using the graphics program "O" (*57*). Where appropriate, manual corrections to the atomic positions were made, and the model was submitted to further cycles of refinement. During the initial steps of structure refinement and density map construction, we noticed a very strong (over 3σ) $F_{obs}-F_{calc}$ electron density that was not explained by the model. Because of the shape presented by this electron density, it was attempted to model it as a fatty acid molecule. As a consequence of its length and geometry, it was modeled as myristic acid, which contains 14 saturated carbons, and for this purpose a minimized model was used to construct a parameter library entry for the program PROTIN using the program MAKEDICT of the CCP4 suite (*58*). The myristic acid molecules (one per subunit) were then incorporated into the model for further refinement with the program REFMAC. Omit maps were calculated using the original dataset and the final refined model devoid of the fatty acid molecules. Water molecules were then introduced using the program ARP (*59*) and included in the final stages of the refinement protocol. Because of a lack of observable density for the final methyl carbon of the myristic acid, this was removed from the model yielding a C_{13} fatty acid that was retained until completion of the refinement. Strict noncrystallographic symmetry was imposed upon the two independent monomers of the asymmetric unit up until the final stages of refinement. At the end of the refinement, the crystallographic *R*-factor had converged to 17.6% (R_{free}= 26.8%). The model was

Table 1: Data Collection and Refinement Statistics

space group	$P2_1$
unit cell	$a = 46.190$
	$b = 60.360$
	$c = 58.740$
	$\beta = 96.05°$
contents of asymmetric unit	1 dimer
resolution (Å)	2.04
completeness (%) (overall/last shell)	90.2/72.5
$I/\sigma(I)$ (overall/last shell)	12.4/2.57
no. of measured reflections	23809
no. of unique reflections	6934
multiplicity	3.433
R_{merge} (overall/last shell)	0.070/0.26
R-factor (%)	17.6
R_{free} factor (%)	26.8
Ramachandran plot (%)	
core region	90.4
additional allowed	7.2
generously allowed	2.4
disallowed	0.0
rms deviation from ideality	
bond lengths (Å)	0.015
bond angles (°)	1.8
WHAT IF quality index (original version)	−1.09
PDB entry	1QLL

evaluated for stereochemical regularity and chemical self-consistency with the programs Procheck (*60*) and What-Check (*61*).

For molecular comparisons, PLA_2 structures were superposed using the least squares options of the graphics program "O" using C_α coordinates only. Where necessary, local superpositions of the calcium binding loop were made using the residues from 23 to 40.

RESULTS

Molecular replacement using a single monomer of the Lys49 PLA_2 from *B. asper* as the search model produced two clear rotation solutions for PrTX-II, with correlation coefficients of 23.6 and 21.6%; these compared with the third highest peak of 11.1%. After translation and rigid body refinement, the correlation coefficient had risen to 63.4% with an *R*-factor of 38.9%. After full refinement, the final *R*-factor and R_{free} were 17.6 and 26.8%, respectively, for a model that includes 1908 protein atoms, two C_{13} saturated fatty acids, and 329 water molecules. The overall stereochemistry of the structure is better than that expected for an average structure at the same resolution (2.04 Å), as indicated by the overall Procheck G-factor of −0.1. No residues were encountered in the disallowed regions of Ramachandran space and only five in the generously allowed regions defined by Procheck. These were residues Leu32 and Asn88 from both monomers and Thr56 from the first monomer. Leu32 forms part of the calcium binding loop described below which is very variable in its conformation within this region. Despite the unusual mainchain torsion angles, the electron density for the leucines at this position in both subunits is clear and unambiguous. Asn88 resides in the loop between the β-wing and the third large α-helix, a frequently problematic region in Lys49 PLA_2 due to poorly defined electron density. In PrTX-II, Asn88 participates in an inverted Asx turn in which its side chain amide is weakly hydrogen bonded to the carbonyl of the glycine two residues previous in the sequence. Furthermore, the carbonyl of the side chain amide is firmly anchored by a hydrogen bond to the mainchain NH group of Ser74, stabilizing the asparagine side chain as it pokes toward the interior of the subunit. Once again, the electron density for Asn88 is clear and unambiguous for both subunits of PrTX-II. The conformation of Thr56 is somewhat different in the two subunits and only presents an unusual combination of φ/ψ angles in the first monomer. This can be accounted for by differences in the crystal contacts for the two monomers. Further quality statistics of the final model can be found in Table 1.

Each of the two monomers of the asymmetric unit present the classical PLA_2 fold shown in Figure 1. The main structural elements are the N-terminal α-helix (helix 1), the "calcium binding loop", two long antiparallel α-helices (2 and 3), the β-wing, and the C-terminal loop. As is often observed in phospholipases A_2, the regions that present the highest temperature factors include the calcium binding loop, the entrance to and exit from the β-wing, and the C-terminal region. The contact region between the two monomers of the asymmetric unit is expected to represent the true dimer interface as it is similar to that described previously for several Lys49 PLA_2 structures (*2*, *46*). The residues involved in the formation of the intersubunit interface are largely

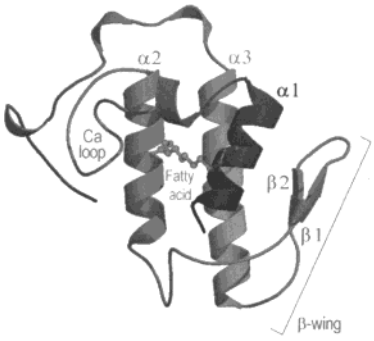

FIGURE 1: Ribbon figure of one monomer of PrTX-I showing the overall fold of the class I/II PLA_2's. The principal elements of secondary structures are identified, as is the β-wing (comprised of two short antiparallel β-strands), the calcium binding loop (present in the D49 PLA_2's), and the bound fatty acid (in ball-and-stick representation). This figure and Figure 4 were produced with the program MOLSCRIPT (*73*).

hydrophilic in nature and are derived from the N-terminal helix and the β-wing. They include the conserved residues Trp77, Glu12, Lys80, Asp79, and Arg107.

As seen in other Lys49 PLA_2 structures, the ϵ-amino group of Lys49 roughly occupies the calcium binding site of the Asp49 active enzymes. It is coordinated via three hydrogen bonds to the mainchain carbonyls of residues 28, 30, and 33, as well as to an apical water molecule. Comparison with other Lys49 PLA_2 structures shows that the exact nature of the interactions formed by the calcium binding loop to the ϵ-amino group are variable as is the mainchain conformation of the loop itself, as shown in Figure 2. This is in sharp contrast to that seen for Asp49 PLA_2, where the essential calcium ion, when present in the crystal structure, is universally coordinated to the mainchain carbonyls of residues 28, 30, and 32 as well as to the side chain of Asp49 and two substitutable water molecules. The substitution of the carbonyl of residue 32 by that of 33 in Lys49 PLA_2 leads to a rearrangement of the exit to the calcium binding loop. This new conformation appears to be stabilized, at least in part, by two hydrogen bonds formed by the side chain amide of Asn28 with the backbone of Gly35, in a manner reminiscent of a β-sheet. Examination of other Lys49 PLA_2 structures shows this to be a conserved feature and appears to serve as a clamp between the entrance and exit to the loop, while permitting considerable conformational variability within the intervening loop itself (Figure 2).

The most notable feature of the electron density map is the presence of unexplained density residing within the hydrophobic channel leading to the active site (Figure 3). This density can be readily interpreted as a free fatty acid, with both of the oxygens of its acidic headgroup hydrogen bonded to a water molecule bound to the catalytic histidine (His48) and one of them accepting a further strong hydrogen bond from the mainchain amide of Gly30. Its hydrocarbon tail extends through the hydrophobic substrate channel to the protein surface. Here it has been built as a C_{13} fatty acid although weak density observable beyond the entrance to the hydrophobic channel suggests that it may possess a longer hydrocarbon chain that is flexible toward its end. In the final model, the *sn*-2 hydrocarbon chain of the fatty acid makes direct apolar contacts with or lies close to several hydrophobic residues including Leu5, Ile9, Gly6, Cys45, Pro18, and Tyr22, which is largely consistent with those observed

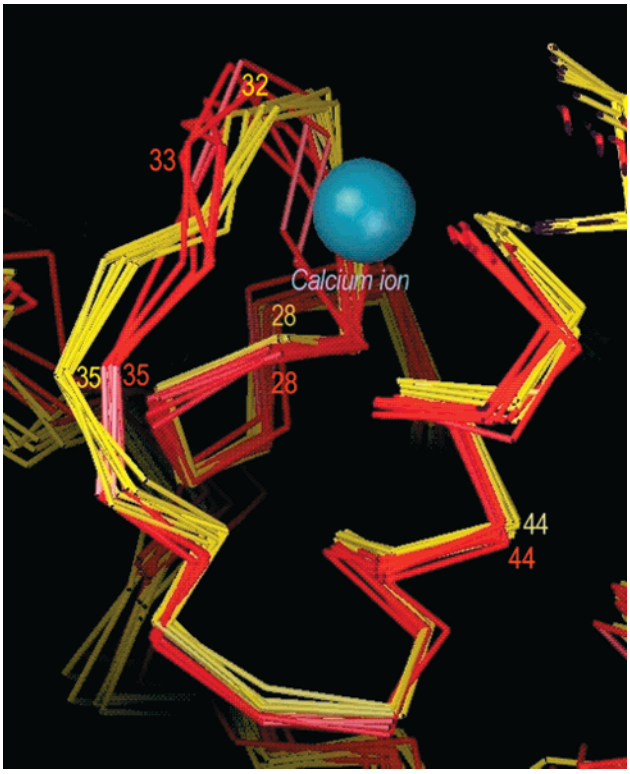

FIGURE 2: The calcium binding loop. α-carbon traces of several PLA_2's are depicted here. All Asp49 structures are shown in yellow and all Lys49 are shown in red. The CPK space filling sphere represents an average position for the calcium ion of the Asp49 structures which varies little as does the structure of the loop itself due to the restraints imposed by calcium binding. The loop structure is a little more variable in the case of the Lys49 structures. The numbers indicate selected residue positions and are color coded accordingly. The PDB structures used were Asp49's: 1VAP (*A. p. piscivorus*), 1PSJ (*A. halys pallas*), 1AYP (human synovial fluid), 1P2P (*Sus scrofa*), 1BP2 (*Bos taurus*), 1POA (*Naja naja atra)* and 1BUN (*Bungarus multicinctus*); Lys49's: 1QLL (*B. pirajai*), 1PPA (*A. piscivorus*), 1GOD (*Cerrophidion godmani*), 1CLP (*B. asper*) and an unpublished structure from *B. jararacussu*, kindly provided by Dr. Raghuvir Arni.

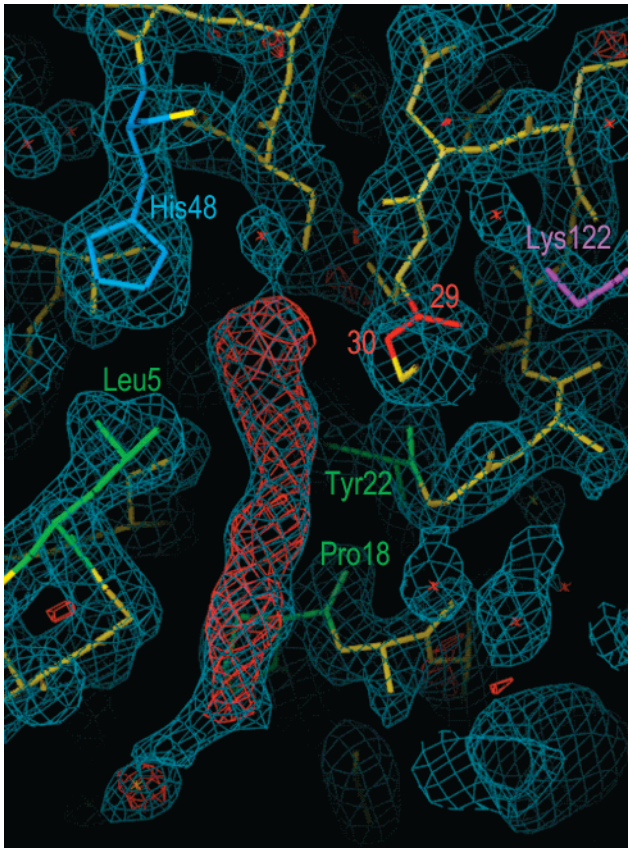

FIGURE 3: Omit map of the fatty acid molecule. $F_{obs}-F_{calc}$ map contoured at 3σ (red) and $2F_{obs}-F_{calc}$ map contoured at 1σ (blue) of the active site region calculated from the final model coordinates excluding the fatty acid. The peptide unit between residues Cys29 and Gly30 which is polarized by Lys122 is depicted in red. His48 is the catalytic histidine and Leu5, Pro18, and Tyr22 form part of the hydrophobic channel.

for the *sn*-2 chain in crystal structures of complexes with phospholipid analogues (*4*, *12*, *16*, *22*).

DISCUSSION

The Lys49 phospholipases A_2 from different species have been shown to present little or no catalytic activity but preserve a membrane damaging capability that leads to diverse pharmacological effects including edema and muscle necrosis (*31*). Over the past few years, many structural studies of such toxins have been reported allowing for a fuller analysis of their similarities and differences as compared with their Asp49 homologues. Crystallographic coordinates were available to us for the Lys49 PLA_2s from *Agkistrodon piscivorus piscivorus* (App) (*39*), *B. asper* (*41*), which has two molecules in the asymmetric unit, *Bothrops jararacussu* [in two different crystal forms, each possessing a dimer in the asymmetric unit (*46*)], *Bothrops (cerrophidion) godmani* (44), and the present dimeric structure, leading to a total of 10 independent crystallographic monomers. A second crystal form of App has also been reported in the literature (*40*) as have structures from *Bothrops nummifer* (*45*), *Bothrops moojeni* (*43*), and for the piratoxin I from *B. pirajai* (*42*), for which coordinates are not yet available. Despite this wealth of structural information, together with related biochemical studies and sequence analyses, the structural basis for myotoxicity and its relationship to reduced or nonexistent catalytic activity remain to be fully elucidated.

An initial proposal for the lack of catalytic activity was made by Scott et al. (*40*) from the crystal structure of App, determined in two crystal forms. It was founded on an earlier proposal from the same group that aimed to establish the structural basis of phopholipase catalysis (*27*). On the basis of several crystal structures of complexes of Asp49 enzymes with a transition state analogue, Scott et al. outlined what has come to be widely regarded as the accepted mechanism (*27*). They point out that on formation of the ES complex, the two water molecules bound to the essential calcium ion are replaced by the oxyanion on the *sn*2 position of the catalytic intermediate and by the *sn*3 phosphate. As such, the latter formally neutralizes the positive charge on the calcium ion, together with its ligand, Asp49. This raises the question of how the negative charge on the oxyanion of the tetrahedral intermediate is sufficiently stabilized for catalysis to occur. Scott et al. suggest that this occurs via a hydrogen bond between the oxyanion and the backbone NH of residue 30, which participates in an unusually polarized peptide bond, due to the presence of a second, auxiliary calcium ion interacting with the carbonyl of Cys29. It was suggested that in structures for which no auxiliary calcium is observed, a

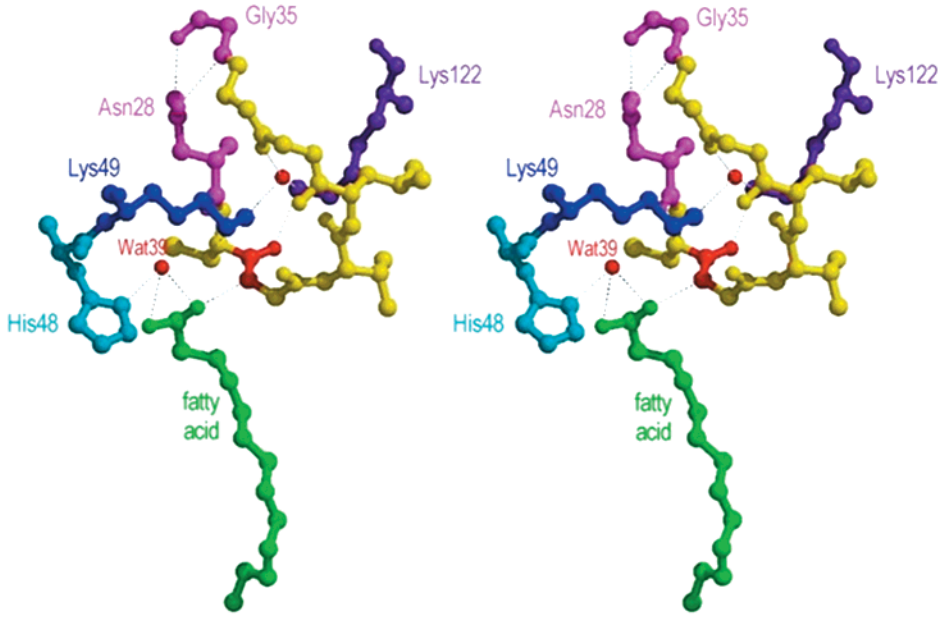

FIGURE 4: Stereoview of the active site. The main elements of the active site are depicted. Lys122 polarizes the peptide unit between Cys29 and Gly30 (red), which strengthens the interaction with the fatty acid headgroup (green). The conformation of Lys49 is stabilized by three hydrogen bonds to the calcium binding loop (not all shown) and to a water molecule that lies between the two lysines (dark blue). Also shown is the interaction between the side chain amide of Asn28 and the backbone of Gly35 (both shown in pink), which forms the clamp linking the two ends of the "calcium binding loop" (in yellow). Water molecules are shown as red spheres.

similar role may be played by Lys122, as in the case of the enzyme from bovine pancreas.

Using this argument, Scott et al. suggest (*40*) that catalysis cannot be supported by Lys49 homologues because the original structure of App showed the peptide between residues 29 and 30 to be flipped, rendering the NH group incapable of stabilizing the oxyanion and the carbonyl unable to interact with an auxiliary positive charge. However, neither this argument nor the original proposal for the need for such a charge has been borne out by subsequent structures. The majority of Asp49 PLA_2's show no auxiliary charge and the majority of Lys49 PLA_2's, including both molecules of the PrTX-II structure reported here, have the peptide bond between 29 and 30 adequately orientated to support catalysis. Although the bovine structure does possess a lysine at position 122, it only weakly interacts with the carbonyl of Cys29, via an intervening water molecule. Furthermore, the more recently solved Asp49 PLA_2 from *A. p. piscivorus*, which also possesses a lysine at position 122, also shows no direct hydrogen bond with Cys29. One example is observed in which the carbonyl of Cys29 forms an H-bond with an alternative basic residue (Arg31 of the Asp49 PLA_2 from *N. naja*), but this structure is calcium-free and therefore probably irrelevant in terms of catalysis.

The observation of a fatty acid molecule bound to both monomers of PrTX-II is reminiscent of that described for the structure of the Lys49 PLA_2 myotoxin I from *B. nummifer* (*45*). In both cases, the fatty acid headgroup forms a hydrogen bond to N30, which in Asp49 active enzymes, stabilizes the oxyanion of the tetrahedral intermediate (*27*). This suggests that the observed fatty acid may be the result of an incomplete catalytic cycle in which there is failure of product release. On the other hand, Pedersen et al. (*35*) have shown that Lys49 PLA_2's, different from Asp49 homologues, will bind free fatty acids, which are not the result of phospholipid hydrolysis. In their studies, they describe the interaction as being made with the fatty acid headgroup and as being covalent in nature although we see no evidence of a covalent bond in the crystal structure of PrTX-II. We suggest that there is still some doubt as to whether the interaction observed by Pedersen et al. was really covalent or not as their conclusion was based principally on gel electrophoresis under denaturing conditions of complexes formed with radio-labeled fatty acids. However, it has been shown for the Lys49 bothropstoxin I that under such conditions, it is not even possible to completely denature the dimer into two monomers (*46*). This casts doubt on whether the conditions used by Pedersen et al. were sufficiently harsh as to ensure complete unfolding, and although the question is still not fully resolved, it seems possible that the fatty acid is secured by a strong noncovalent interaction rather than a covalent bond. This is supported by our structure in which the absence of bridging density from the fatty acid to N30 as well as the average N−O interatomic separation of 2.70 Å for the two monomers suggest a hydrogen bond.

The presence of the bound fatty acid may help to rationalize what has always been a puzzling aspect of Lys49 PLA_2 structure, namely, the complete conservation of the residues involved in catalysis. This suggests that the fatty acid may be the result of phospholipid hydrolysis by PrTX-II (albeit conceivably with reduced efficiency) followed by a failure of product release. This would lead to enzyme inhibition and may explain the failure of many attempts to measure catalytic activity for Lys49 PLA_2 in vitro using standard assays (*40*, *62*−*64*), since the enzyme would either be naturally inhibited after an encounter with phospholipid or free fatty acid during purification or become so after one cycle of catalysis during the enzyme assay.

The fact that bound fatty acids have thus far only been observed in two crystal structures of PLA_2, both Lys49 homologues (PrTX-II and the myotoxin I from *B. nummifer*),

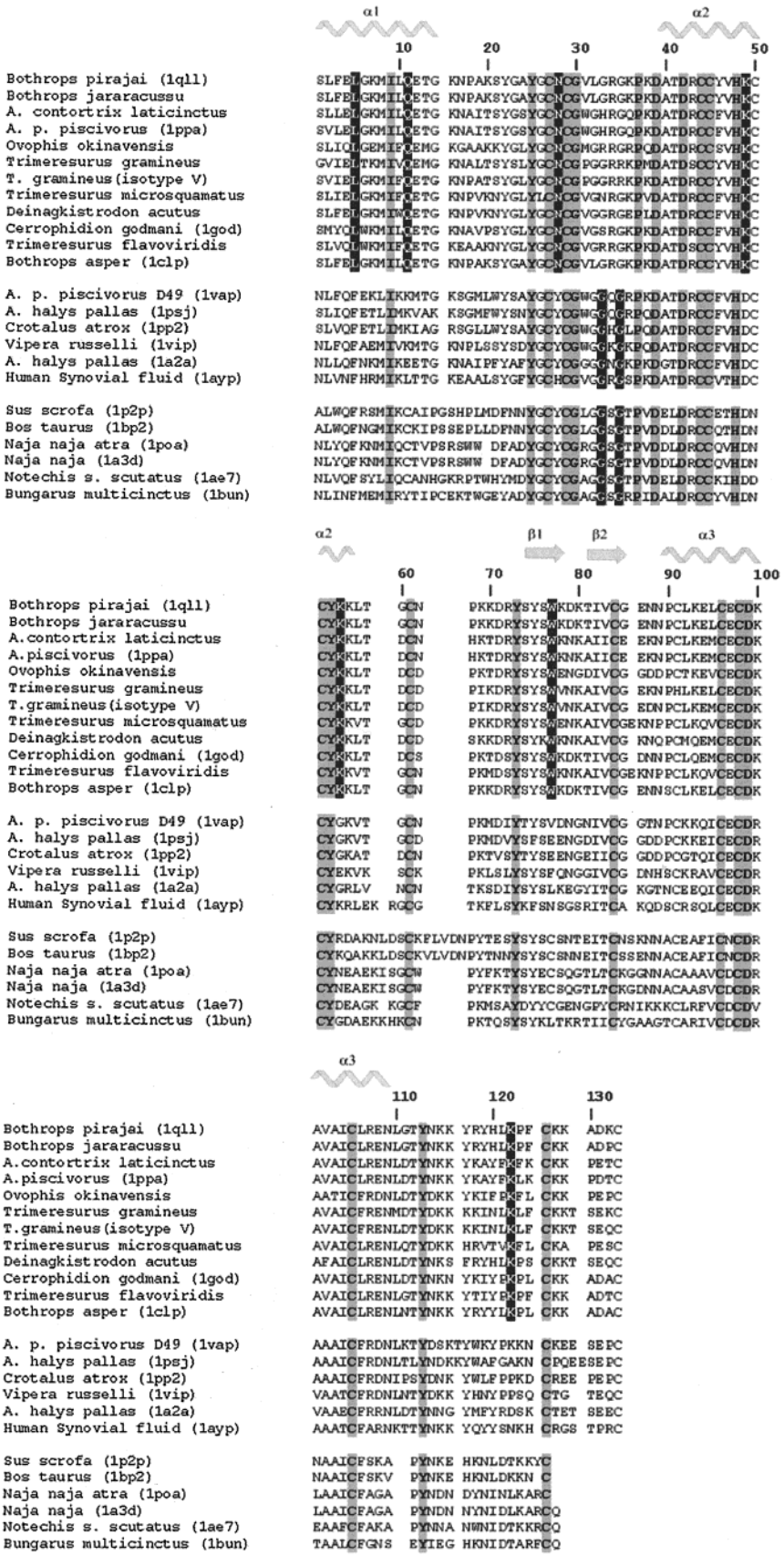

FIGURE 5: Sequence comparison of PLA_2's. Multiple alignment of different PLA_2's produced by the MULTALIGN program (*74*) with adjustments based on structural superpositions. The sequences have been numbered according to Renetseder et al. (*29*) based on the sequence of the enzyme from bovine pancreas. The sequences were grouped into three categories: class II Lys49/Lys122 PLA_2's and classes II and I Asp49 PLA_2's, respectively. In the latter two categories, only sequences of known three-dimensional structure have been included. The species pertinent to each sequence is indicated on the left, followed by its corresponding PDB ID code (where appropriate). Grey shaded amino acids denote residues that are conserved in all three categories. Black boxes denote conserved residues in either one or more of the three categories and are commented on in the text. The secondary structure for *B. pirajai* piratoxin-II is represented over the alignment.

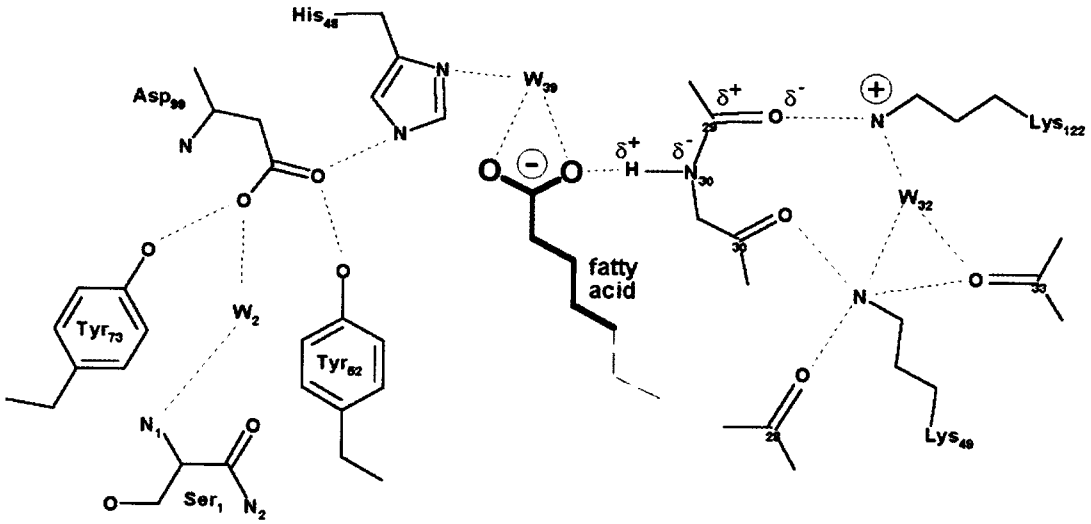

FIGURE 6: Generalized schematic drawing of the active site of Lys49 PLA_2's. To the left of the fatty acid are shown the principal components of the highly conserved catalytic machinery. On the right, Lys49 and the backbone carbonyls from the "calcium binding loop" are shown together with the polarized peptide bond and Lys122.

together with the studies of Pedersen et al., which showed fatty acid binding exclusively to Lys49 homologues, deserves comment. What is the structural origin of the high affinity for fatty acid in Lys49 homologues that leads to a failure of product release?

From the crystal structure of both subunits of PrTX-II, it can be seen that the peptide bond between Cys29 and Gly30 is expected to be unusually polarized due to the presence of the buried Lys122 interacting with the carbonyl of Cys29 (Figure 4). As originally proposed by Scott et al. (*27*), this would lead to a hyperpolarization of the peptide bond, focusing positive charge on the fatty acid carboxylate, impeding its release.

Of the ten Lys49 monomer structures available, seven present this interaction, and there are good reasons why the remaining three do not. In the closed conformation of bothropstoxin I, as a consequence of crystal packing in one of the subunits Lys122 points out toward the solvent due to a significant alteration to the conformation of the C-terminus. However, the viability of the interaction is clear from its presence in the remaining monomer of the closed conformation and in both monomers of the open conformation (*46*). In the case of one of the crystal forms of App (*39*, *40*) and the *B. godmani* structure, the interaction is not observed due to an altered conformation of part of the calcium binding loop. Once again, it is likely that the Lys122−Cys29 interaction is viable in this case as the deformation to the calcium binding loop is not observed in the second crystal form of App (*40*).

Once bound to the PLA_2, the fatty acid may serve as a hydrophobic anchor aiding in the insertion of the protein into the phospholipid membrane and allowing the manifestation of toxic effects possibly via independent sites on the molecule as has been frequently suggested (*38*, *41*, *62*, *65*−*67*). A similar mechanism of protein binding to cell membranes has been described previously, particularly for myristoylated proteins. Nonspecific electrostatic interaction between basic motifs in the proximity of the fatty acid with acidic cell membranes also occurs in these proteins (*68*). These motifs are responsible, along with the fatty acid anchor, for effective binding to membranes, since the fatty acids by themselves are generally not sufficient to ensure stable anchoring (*69*, *70*, *71*). As well as a fatty acid anchor, PrTX-II also displays an electropositive area near the cleft where the fatty acid is found, a finding that supports a binding mechanism similar to that described above.

Recent experimental evidence (*36*, *37*) has demonstrated that two Lys49 PLA_2's isolated from the venom of the Habu snake (*Trimeresurus flavoviridis*) as well as App and myotoxin II from *B. asper* show considerable enzymatic activity in liberating arachidonate from 2-arachidonoyl-1-stearoyl-L-3-phosphatidylcholine (ASPC) liposomes. This is supported by other recent studies using different Lys49 toxins (*72*). It is possible therefore that the phenomenon of product release may turn out to be fatty acid-specific. At the very least, it seems clear that the presence of Lys49 is not per se sufficient for a lack of phospholipolytic activity. The apparent flexibility of the "Ca^{2+}-binding loop" in Lys49 enzymes, evidenced by the limited degree of variability shown in Figure 2, suggests the possibility that Lys49 may be able to simulate the role of the Ca^{2+} ion by temporarily releasing two of its carbonyl or water ligands to accommodate a phospholipid substrate and, together with NH30, stabilize the oxyanion of the intermediate sufficiently to allow catalysis to proceed, albeit at a conceivably reduced rate.

Figure 5 shows that Lys122 is absolutely conserved in all Lys49 PLA_2 but rare in Asp49 enzymes consistent with the fundamental role we propose. If Asp49 PLA_2 enzymes were to possess such an interaction, it is possible that they would become rapidly product-inhibited, a hypothesis that could be tested by site-directed mutagenesis. Figure 6 shows a schematic representation of the active site showing the most important interactions involved, including the polarization of the essential peptide bond by Lys122. Figure 5 also highlights both absolute conservations and residues characteristic of either Lys49 or Asp49 sequences. Several of these have been described in recent analyses (*38*, *67*), but it is curious that the importance of Lys122 has heretofore remained uncommented on. The side chain of Asn28, conserved in all Lys49 sequences, forms the clamp between the entrance and the exit to the calcium binding loop. This leads to a rearrangement to the structure of the exit from

the loop that releases somewhat the conformational constraint on Gly33 and Gly35, which are less well-conserved in the case of the Lys49 enzymes (Figure 5).

In conclusion, we have suggested that an alternative explanation for the lack of phospholipase activity observed in vitro for Lys49 PLA_2's is their strong binding affinity for the fatty acid product. Paradoxically, such enzymes may therefore be both "active", in that they may be capable of hydrolysis (which would explain the conservation of the catalytic machinery) but frequently also "inactive" in vitro, due to inhibition as a result of failure of product release. This is by no means meant to imply that product inhibition is the only source of reduced activity as Lys49 is not expected to support catalysis with the same efficiency as Ca^{2+} (*24*). We can also not completely rule out the possibility that Lys49 PLA_2 are simply fatty acid binding proteins that are unable to catalyze phospholipid hydrolysis. However, recent experimental data on arachidonate release from ASPC liposomes seems to disfavor this hypothesis (*36*, *37*).

It is ironical that the original proposal of Scott et al. (*27*) for the need for an auxiliary electrophile for catalytic activity in active phospholipases, and the suggestion that this may be Lys122 for many such molecules, may in reality turn out to be the exact opposite. Lys122 is in fact rarely present in active Asp49 PLA_2's but is absolutely conserved in the "inactive" Lys49 homologues thus far sequenced. We propose that the polarization of the peptide bond between residues 29 and 30 by Lys122 is the principal reason for the high affinity of Lys49 PLA_2's for fatty acid and which consequently leads to enzyme inhibition. We therefore recommend that henceforth such molecules be referred to as Lys49/Lys122 PLA_2's in recognition of the important role played by both lysine residues.

ACKNOWLEDGMENT

We are grateful to Drs. Raghuvir Arni and Richard Ward for useful discussions and for providing access to unpublished data.

REFERENCES

1. Arni, R. K., and Ward, R. J. (1996) *Toxicon 34*, 827−841.
2. Ward, R. J., de Azevedo, W. F., Jr., and Arni, R. K. (1998) *Toxicon 36*, 1623−1633.
3. Brunie, S., Bolin, J., Gewirth, D., and Sigler, P. B. (1985) *J. Biol. Chem. 260*, 9742−9749.
4. White, S. P., Scott, D. L., Otwinowski, Z., Gelb, M. H., and Sigler, P. B. (1990) *Science 250*, 1560−1563.
5. Zhao, K., Song, S., Lin, Z., and Zhou, Y. (1998) *Acta Crystallogr. D54*, 510−521.
6. Carredano, E., Westerlund, B., Persson, B., Saarinen, M., Ramaswamy, S., Eaker, D., and Eklund, H. (1998) *Toxicon 36*, 75−92.
7. Kwong, P. D., McDonald, N. Q., Sigler, P. B., and Hendrickson, W. A (1995) *Structure 3*, 1109−1119.
8. Han, S. K., Yoon, E. T., Scott, D. L., Sigler, P. B., and Cho, W. (1997) *J. Biol. Chem. 272*, 3573−3582.
9. Wang, X., Yang, J., Gui, L., Lin, Z., Chen, Y., and Zhou, Y. (1996) *J. Mol. Biol. 255*, 669.
10. Tang, L., Zhou, C., and Lin, Z. J. (1998) *J. Mol. Biol. 282*, 1−11.
11. Segelke, B. W., Nguyen, D., Chee, R., Xuong, N. H., and Dennis, E. A (1998) *J. Mol. Biol. 279*, 223−232.
12. Scott, D. L., Otwinowski, Z. Gelb, M. H., and Sigler, P. B. (1990) *Science 250*, 1563−1566.
13. Dijkstra, B. W., Kalk, K. H., Hol, W. G. J., and Drenth, J. (1981) *J. Mol. Biol. 147*, 97−123.
14. Dijkstra, B. W., Renetseder, R., Kalk, K. H., Hol, W. G. J., and Drenth, J. (1983) *J. Mol. Biol. 168*, 163−179.
15. Wery, J.-P., Schevitz, R. W., Clawson, D. K., Bobbitt, J. L., Dow, E. R., Gamboa, G., Goodson, T., Jr., Hermann, R. B., Kramer, R. M., McClure, D. B., Mehelich, E. D., Putnam, J. E., Sharp, J. D., Stark, D. H., Teater, C., Warrick, M. W., and Jones, N. D. (1991) *Nature 352*, 79−82.
16. Scott, D. L., White, S. P., Browning, J. L., Rosa, J. J., Gelb, M. H., and Sigler, P. B. (1991) *Science 254*, 1007−1010.
17. van den Berg, B., Tessari, M., de Haas, G. H., Verheij, H. M., Boelens, R., and Kaptein, R. (1995) *EMBO J. 14*, 4123−4131.
18. van den Berg, B., Tessari, M., Boelens, R., Dijkman, R., de Haas, G. H., Kaptein, R., and Verheij, H. M. (1995) *Nat. Struct. Biol. 2*, 402−406.
19. Gelb, M. H., Jain, M. K., Hanel, A. M., and Berg, O. G. (1995) *Annu. Rev. Biochem. 64*, 653−688.
20. Zhou, F., and Schulten, K. (1996) *Proteins: Struct. Funct. Genet. 25*, 12−27.
21. Schevitz, R. W., Bach, N. J., Carlson, D. G., Chirgadze, N. Y., Clawson, D. K., Dillard, R. D., Draheim, S. E., Hartley, L. W., Jones, N. D., Mihelich, E. D., Olkowski, J. L., Snyder, D. W., Sommers, C., and Wery, J-P. (1995) *Nat. Struct. Biol. 2*, 458−465.
22. Thunnissen, M. M. G. M., AB, E., Kalk, K. H., Drenth, J., Dijkstra, B. W., Kuipers, P., Dijkman, R., de Haas, G. H., and Veiheij, H. M. (1990) *Nature 689*, 689−691.
23. Sekar, K., Yu, B.-Z., Rogers, J., Lutton, J., Liu, X., Chen, X., Tsai, M.-D., Jain, M. K., and Sundaralingam, M. (1997) *Biochemistry 36*, 3104−3114.
24. Liu, X., Zhu, H., Huang, B., Rogers, J., Yu, B.-Z., Kumar, A, Jain, M. K., Sundaralingam, M., and Tsai, M.-D. (1995) *Biochemistry 34*, 7322−7334.
25. Li, Y., Yu, B.-Z., Zhu, H., Jain, M. K., and Tsai, M−D. (1994) *Biochemistry 33*, 14714−14722.
26. Veiheij, H. M., Volwerk, J. J., Jansen, E. H. J. M., Puyk, W. C., Dijkstra, B. W., Drenth, J., and de Haas, G. H. (1980) *Biochemistry 19*, 743−750.
27. Scott, D. L., White, S. P., Otwinowski, Z., Yuan, W., Gelb, M. H., and Sigler, P. B. (1990) *Science 250*, 1541−1546.
28. Blow, D. M., Birktoft, J. J., and Hartley, B. S. (1969) *Nature 221*, 337−340.
29. Renetseder, R., Brunie, S., Dijkstra, B. W., Drenth, J., and Sigler, P. B. (1985) *J. Biol. Chem. 260*, 11627−11636.
30. Rogers, J., Yu, B.-Z., Serves, S. V., Tsivgoulis, G. M., Sotiropoulos, D. N., Ioannou, P. V., and Jain, M. K. (1996) *Biochemistry 35*, 9375−9384.
31. Gutiérrez, J. M., and Lomonte, B. (1995) *Toxicon 33*, 1405−1424.
32. Maraganore, J. M., Merutka, G., Cho, W., Welches, W., Kezdy, F. J., and Heinrikson, R. L. (1984) *J. Biol. Chem. 259*, 13839−13843.
33. van den Bergh, C. J., Slotboom, A. J., Verheij, H. M., and de Haas, G. H. (1989) *J. Cell. Biochem. 39*, 379−390.
34. Homsi-Brandeburgo, M. I., Queiroz, L. S., Santo-Neto, H., Rodrigues-Simioni, L., and Giglio, J. R. (1988) *Toxicon 26*, 615−627.
35. Pedersen, J. Z., Lomonte, B., Massoud, R., Gubenšek, F., Gutiérrez, J. M., and Rufini, S. (1995) *Biochemistry 34*, 4670−4675.
36. Shimohigashi, Y., Tani, A., Matsumoto, H., Nakashima, K., Yamaguchi, Y., Oda, N., Takano, Y., Kamiya, H., Kishino, J., Arita, H., and Ohno, M. (1995) *J. Biochem. 118*, 1037−1044.
37. Yamaguchi, Y., Shimohigashi, Y., Chiwata, T., Tani, A., Chijiwa, T., Lomonte, B., and Ohno, M. (1997) *Biochem. Mol. Biol. Int. 43*, 19−26.
38. Ward, R. J., Rodrigues, Alves, R., Ruggiero Neto, J., Arni, R. K., and Casari, G. (1998) *Protein Eng. 11*, 285−294.
39. Holland, D. R., Clancy, L. L., Muchmore, S. W., Ryde, T. J., Einspahr, H. M., Finzel, B. C., Heinrikson, R. L., and Watenpaugh, K. D. (1990) *J. Biol. Chem.* 265, 17649−17656.

40. Scott, D. L., Achari, A., Vidal, J. C., and Sigler, P. B. (1992) *J. Biol. Chem. 267*, 22645−22657.
41. Arni, R. K., Ward, R. J., Gutiérrez, J. M., and Tulinsky, A. (1995) *Acta Crystallogr. D51*, 311−317
42. de Azevedo, W. F., Jr.., Ward, R. J., Canduri, F., Soares, A., Giglio, J. R., and Arni, R. K. (1998) *Toxicon 36*, 1395−1406.
43. de Azevedo, W. F., Jr., Ward, R. J., Lombardi, F. R., Giglio, J. R., Soares, A. M, Fontes, M. R. M., and Arni, R. K. (1997) *Protein Pep. Lett. 4*, 329−334.
44. Arni, R. K., Fontes, M. R. M., Barberato, C., Gutiérrez, J. M., Díaz, C., and Ward, R. J. (1999) *Arch. Biochem. Biophys. 366*, 177−182.
45. de Azevedo, Jr. W. F., Ward, R. J., Gutiérrez, J. M., and Arni, R. K. (1999) *Toxicon 37*, 371−384.
46. da Silva Giotto, M. T., Garratt, R. C., Oliva, G., Mascarenhas, Y. P., Giglio, J. R., Cintra, A. C. O., de Azevedo Jr., W. F., Arni, R. K., and Ward, R. J. (1998) *Proteins: Struct. Funct. Genet. 30*, 442−454.
47. Toyama, M. H., Mancuso, L. C., Giglio, J. R., Novello, J. C., Oliveira, B., and Marangoni, S. (1995) *Biochem. Mol. Biol. Int. 37*, 1047−1055.
48. Jancarik, J., and Kim, S. H. (1991) *J. Appl. Cryst. 24*, 409−411.
49. Lee, W. H., Gonçalez, M. C., Ramalheira, R. M. F., Kuser, P. R., Toyama, M. H., Oliveira, B., Giglio, J. R., Marangoni, S., and Polikarpov, I. (1998) *Acta Crystallogr. D54*, 1437−1439.
50. Polikarpov I., Oliva, G., Castellano, E. E., Garratt, R. C., Arruda, P., Leite, A., and Craievich, A. (1998) *Nucl. Inst. Methods Phys. Res.* A *405*, 159−164.
51. Polikarpov, I., Perles, L. A., de Oliveira, R. T., Oliva, G., Castellano, E. E., Garratt, R. C., and Craievich, A. (1998) *J. Synch. Rad.* 5, 72−76.
52. Otwinowski, Z., and Minor, W. (1997) *Methods Enzymol. 276*, 307−326.
53. Navaza, J. (1994) *Acta Crystallogr. A50*, 157−163.
54. Murshudov, G. N., Vagin, A. A., and Dodson, E. J. (1997) *Acta Crystallogr. D53*, 240−255.
55. Toyama, M. H., Soares, A. M., Novello, J. C., Oliveira, B., Giglio, J. R., Lee, W.-H., Polikarpov, I., and Marangoni, S. (2000) *Biochimie*, in press.
56. Brunger, A. T. (1992) *Nature 355*, 472−474.
57. Jones, T. A., Zou, J.-Y., Cowan, S. W., and Kjeldgaard, M. (1991) *Acta Crystallogr. A47*, 110−119.
58. Collaborative Computational Project Number 4 (1994) *Acta Crystallogr. D50*, 760−763.
59. Lamzin, V. S., and Wilson, K. S. (1993) *Acta Crystallogr. D49*, 129−147.
60. Laskowski, R. A., MacArthur, M. W., Moss, D. S., and Thornton, J. M. (1993) *J. Appl. Cryst. 26*, 283−291.
61. Hooft, R. W. W., Vriend, G., Sander, C., and Abola, E. E. (1996) *Nature 381*, 272−272.
62. Francis, B., Gutierrez, J. M., Lomonte, B., and Kaiser, I. I. (1991) *Arch. Biochem. Biophys. 284*, 352−359.
63. van den Bergh, C. J., Slotboom, A. J., Verheij, H. M., and de Haas, G. H. (1988) *Eur. J. Biochem. 176*, 353−357.
64. Condrea, E. (1989) *Toxicon 27*, 705−706.
65. Kini, R. M., and Iwanaga, S. (1986) *Toxicon 24*, 895−905.
66. Lomonte, B., Moreno, E., Tarkowski, A., Hanson, L. Å. (1994) *J. Biol. Chem. 269*, 29867−29873.
67. de Araujo, H. S. S., White, S. P., and Ownby, C. L. (1996) *Arch. Biochem. Biophys. 326*, 21−30.
68. Murray, D., Ben-Tal, N., Honig, B., and McLaughin, S. (1997) *Structure 5*, 985−989.
69. Resh, M. D. (1996) *Cell. Signaling 8*, 403−412.
70. Bhatnagar, R. S., and Gordon, J. I. (1997) *Trends Cell Biol. 7*, 14−21.
71. Xu, W., Harrison, S. C., and Eck, M. J. (1997) *Nature 385*, 595−602.
72. Fletcher, J. E., and Jiang, M-S. (1998) *Toxicon 36*, 1549−1555.
73. Kraulis, P. J. (1991) *J. Appl. Crystallogr. 24*, 946−950.
74. Barton, G., and Sternberg, M. J. E. (1987) *J. Mol. Biol. 198*, 327−337.

BI0010470